CHAPTER IV

VOLTAGE DEVIATION IMPROVEMENT IN ACTIVE DISTRIBUTION NETWORK USING BETTERY ENERGY STORAGE SYSTEM OPTIMAL VOLTAGE DROOP CONTROL

4.1 Introduction

From Chapter 3, once the voltage stability of the system has been assessed using the L-index, which is a tool capable of identifying weak buses, the weak buses identified by the L-index become the locations where BESS is installed. This chapter proposes methods for voltage control to enhance system stability and reliability. In section 2.5, there are three methods of voltage control: STATCOM, capacitor banks, and tap-changing transformers. Each method has its own advantages and disadvantages but is still not suitable for systems with renewable energy, as such systems require energy storage and the ability to supply or absorb real power. Therefore, in section 2.6 and 2.7, a method of voltage control using BESS is proposed.

This study provides a way to solve the impact of renewable energy on VD of the Active Distribution Network (AND). The optimum BESS management is achieved by adopting a Voltage Droop Control (VDC) approach that employs BESS to charge and discharge energy into the system. The adaptive droop control approach was chosen for BESS management because it allows the droop coefficient to be chosen as desired and appropriate, as well as taking into account the SoC level. In addition, the PSO is used to get the most appropriate droop coefficient value for battery control. The IEEE 33-bus test system was chosen as a test system because it is a distribution system with voltage levels lower than the standard criterion, making it acceptable for testing.

4.2 BESS with Adaptive Droop Control

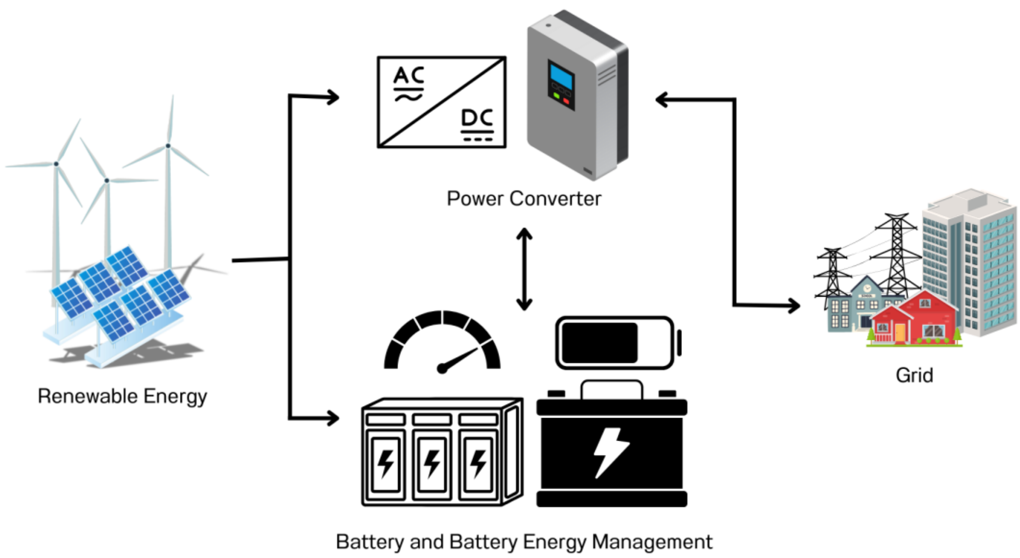

Figure. 4.1 BESS configuration

The BESS configuration is shown in Fig. 4.1, which includes the following main elements: a battery for storing energy, a battery energy management system for controlling BESS operation, and a power converter for energy conversion.

In this study, we focus on the battery and its energy management system. This study presents a method for controlling battery operations to resolve the VD issue. The battery can either provide or receive active power from the grid. When the BESS supplies active power to the grid, the voltage level rises, whereas when it absorbs active power from the grid, the voltage level drops. Thus, the BESS's operation can affect the voltage when the active power changes. Therefore, effective BESS operation relies heavily on battery energy management. According to a review, Fig. 4.2 shows that the VDC has three modes: (1) Mode 1 (Fixed Voltage): Keeps the voltage at a predetermined level and allows the battery power to adjust as needed, (2) Mode 2 (Fixed Power): Keeps the battery's power output constant, (3) Mode 3 (Droop Control): Uses a droop coefficient to determine how much power the battery delivers or consumes depending on the grid voltage.

This study uses the droop control method (Mode 3) to regulate battery operation because it can adjust the droop coefficient, allowing the voltage level to be freely regulated. Fig. 4.3 illustrates the operating concept as follows:

• 1: If the bus voltage of the battery exceeds the maximum voltage ($V_{\max}$), the battery will charge the maximum power into the system.

• 2: If the bus voltage value of the battery is less than the maximum voltage ($V_{\max}$) but larger than the maximum voltage thresholds ($V_{\text{th}}^{\max}$), the battery will charge power based on VD, which is governed by the droop coefficient.

• 3: If the battery's bus voltage value falls within the range of the minimum voltage thresholds ($V_{\text{th}}^{\min}$) and the maximum voltage thresholds ($V_{\text{th}}^{\max}$) or the deadband range, the battery will not charge or discharge at all.

• 4: If the bus voltage value of the battery is larger than the minimum voltage ($V_{\min}$) but less than the minimum voltage thresholds ($V_{\text{th}}^{\min}$), the battery will discharge the power based on VD, which is governed by the droop coefficient.

• 5: If the battery's bus voltage value is less than the minimum voltage ($V_{\min}$), it will discharge the maximum power back.

It can be represented mathematically as an equation given below:

$$P_{BES} = \begin{cases} -P_{BES}^{\max} & \text{if } V_k \geq V^{\max} \\ k_{BES,c(SoC)}\Delta V & \text{if } V_{\text{th}}^{\max} < V_k < V^{\max} \\ 0 & \text{if } V_{\text{th}}^{\min} \leq V_k \leq V_{\text{th}}^{\max} \\ k_{BES,d(SoC)}\Delta V & \text{if } V^{\min} < V_k < V_{\text{th}}^{\min} \\ P_{BES}^{\max} & \text{if } V_k \leq V^{\min} \end{cases} \tag{4.1}$$

$$\Delta V = V_k - V_0 \tag{4.2}$$

Since the battery may be saturated, it cannot be utilized further, causing the system to have a VD value that exceeds the required limit. As a result of the investigation, the SoC level was examined, as shown in the equation below.

$$k_{BES,d} = \begin{cases} 0 & \text{if } 0 < \text{SoC} \leq \text{SoC}_{\min} \\ \dfrac{K_{\max} K_{\min} e^{n_d (SoC - SoC_{\min})}}{K_{\max} + K_{\min} e^{n_d (SoC - SoC_{\min})} - 1} & \text{if } \text{SoC}_{\min} < \text{SoC} \leq 1 \end{cases} \tag{4.3}$$

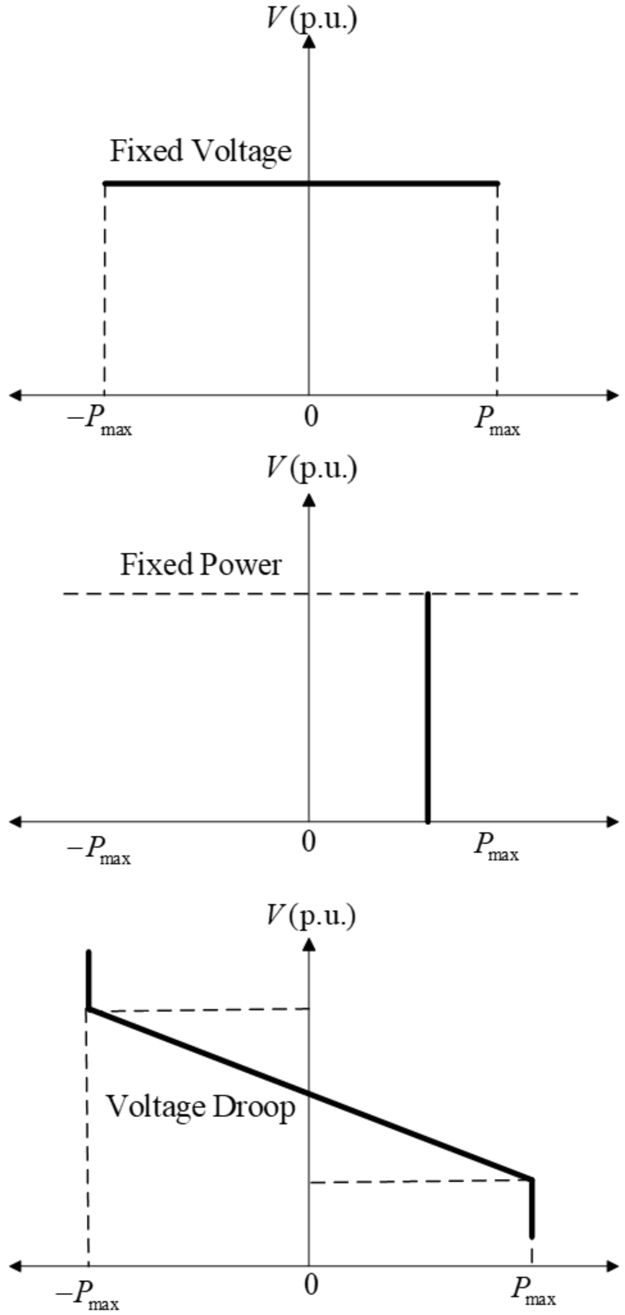

Figure 4.2 VDC strategies

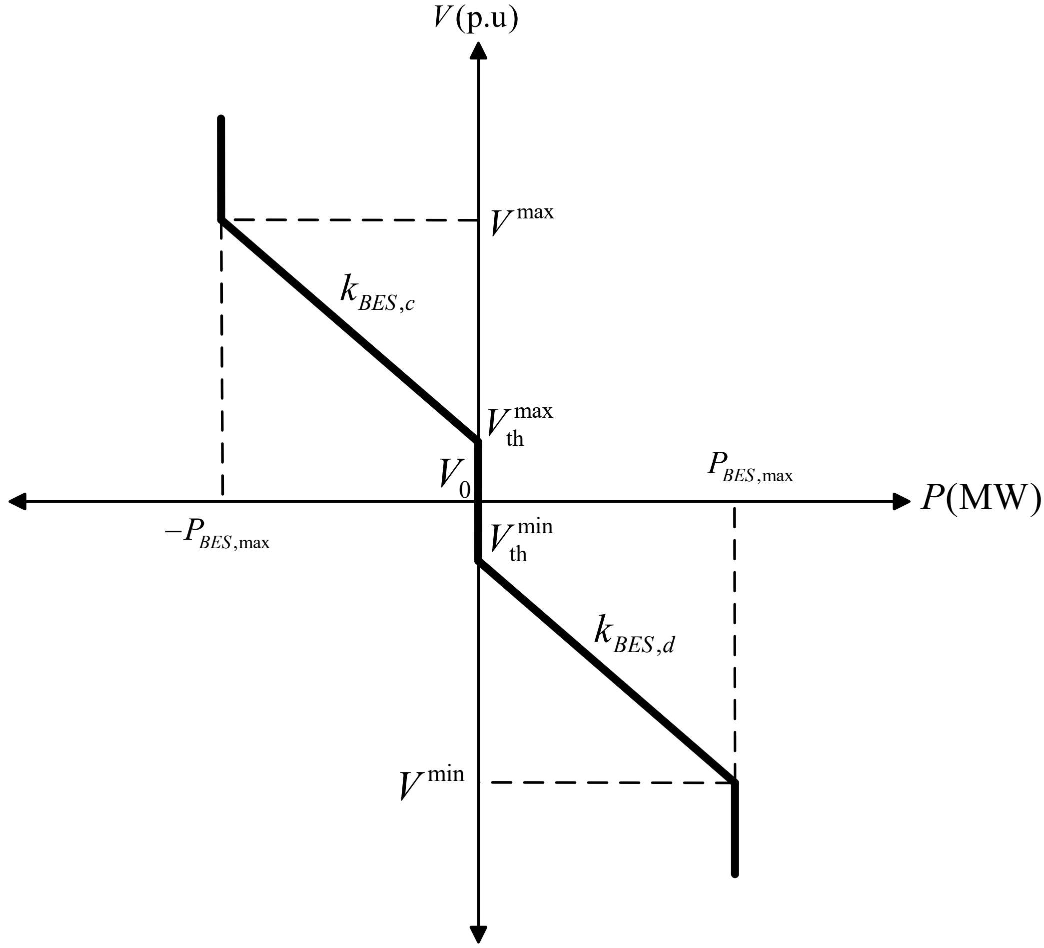

Figure 4.3 Adaptive VDC strategy

$$k_{BES,c} = \begin{cases} 0 & \text{if } \mathrm{SoC}_{\max} \le \mathrm{SoC} < 1 \\ \dfrac{K_{\max} K_{\min} e^{n_c(SoC_{\max} - SoC)}}{K_{\max} + K_{\min} e^{n_c(SoC_{\max} - SoC)} - 1} & \text{if } 0 < \mathrm{SoC} < \mathrm{SoC}_{\max} \end{cases} \tag{4.4}$$

$$SoC(t) = SoC(t-1) - \frac{1}{E} \int P_{BES}(t) dt \tag{4.5}$$

$$k_{droop} = \begin{cases} k_{BES,c}, & \text{charging} \\ k_{BES,d}, & \text{discharging} \end{cases} \tag{4.6}$$

$$n = \begin{cases} n_c, & \text{charging} \\ n_d, & \text{discharging} \end{cases} \tag{4.7}$$

The control of the BESS using VDC can be modeled into the Newton-Raphson load flow analysis through the following equations:

$$P_{BES} + P_k^{gen} - P_k^{load} - \sum_{j=1}^{n}[V_k V_j (G_{ij}\cos\theta_{ij} + B_{ij}\sin\theta_{ij})] = 0 \quad (4.8)$$

As shown in Equation (4.8), the real power output of the BESS, denoted as P_{BES}, which is obtained from the VDC strategy, is incorporated into the NRLF's power equations. This allows for the calculation of bus voltages after the contribution from the BESS has been integrated into the system. A negative P_{BES} value indicates that the battery is charging, while a positive P_{BES} value indicates that the battery is discharged.

When evaluating k_{droop}, it is discovered that this value is related to the determination of $K_{\max}$, $K_{\min}$, SoC, and n As a result, while examining (4.1), (4.3), and (4.4), it can be represented in Fig. 4.4 and 4.5. From Fig. 4.4, it has been discovered that as the SoC of the battery increase, the $k_{BES,d}$ value gradually increases, the $k_{BES,c}$ value gradually decrease. This is because adaptive droop management is intended to protect the battery's functionality, which increases the SoC range, resulting in less charging and discharging. On the other hand, a low SoC level in the battery causes it to charge more and discharge less. The aforementioned relationship leads to the design of $K_{\max}$, $K_{\min}$ and n values, demonstrating that $K_{\max}$ and $K_{\min}$ will have a relationship with the desired power output, and n will be the factor determining the battery's power distribution, which is related to SoC, as shown in Fig. 4.5.

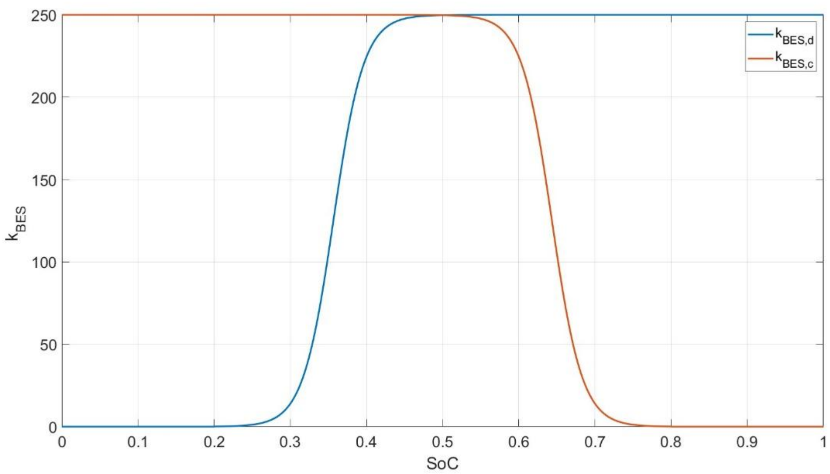

Figure 4.4 The Relationship between SoC and k_{BES} with the SoC is within the range of $SoC_{\min}$ and $SoC_{\max}$

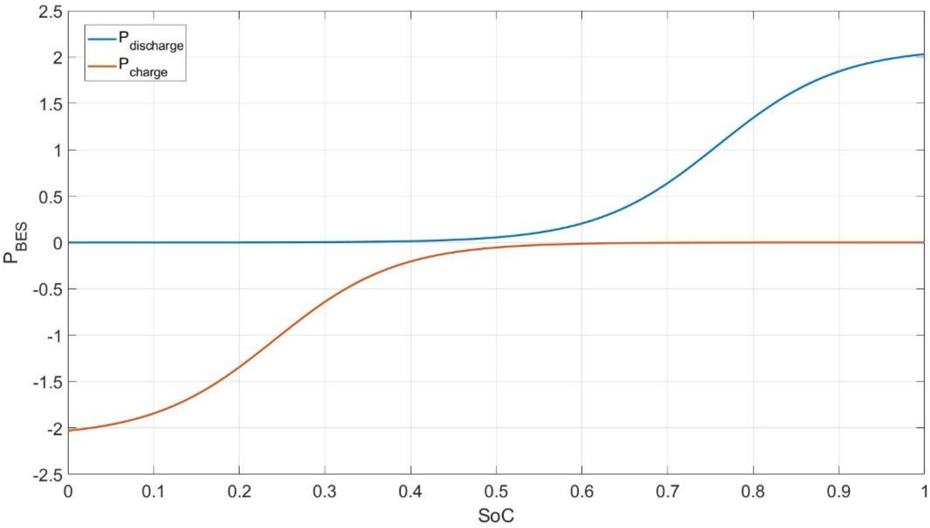

Figure 4.5 The Relationship between SoC and n with the SoC is within the range of $SoC_{\min}$ and $SoC_{\max}$

4.3 PSO Based Voltage Deviation Improvement

This study aims to minimize the system's total voltage deviation (TVD) through the objective function. By reducing the TVD, the stability of the power system can be greatly enhanced. The objective function employed in this study is shown in the following equation.

$$\text{minimize } TVD = \sum_{k=1}^{N}(|V_k - V_0|) \tag{4.9}$$

and the constraints are defined as follows:

$$P_k^{gen} - P_k^{load} - \sum_{j=1}^{n}[V_k V_j (G_{kj}\cos\theta_{kj} + B_{kj}\sin\theta_{kj})] = 0 \tag{4.10}$$

$$Q_k^{gen} - Q_k^{load} - \sum_{j=1}^{n}[V_k V_j (G_{kj}\sin\theta_{kj} - B_{kj}\cos\theta_{kj})] = 0 \tag{4.11}$$

$$V_{\min} \le V_k \le V_{\max} \tag{4.12}$$

$$SoC_{\min} \le SoC \le SoC_{\max} \tag{4.13}$$

$$P_{BES,\min} \le P_{BES} \le P_{BES,\max} \tag{4.14}$$

$$k_{BES,d}^{\min} \le k_{BES,d} \le k_{BES,d}^{\max} \tag{4.15}$$

$$k_{BES,c}^{\min} \le k_{BES,c} \le k_{BES,c}^{\max} \tag{4.16}$$

The working equation of PSO is as follows Eq. (3.12) and Eq. (3.13).

where x_i is the population of particles that represent the adjust exponent of $k_{BES,d}$ and $k_{BES,c}$, which are n_d and n_c, respectively. The proposed PSO-based VD improvement computational procedure is illustrated in Fig 4.6.

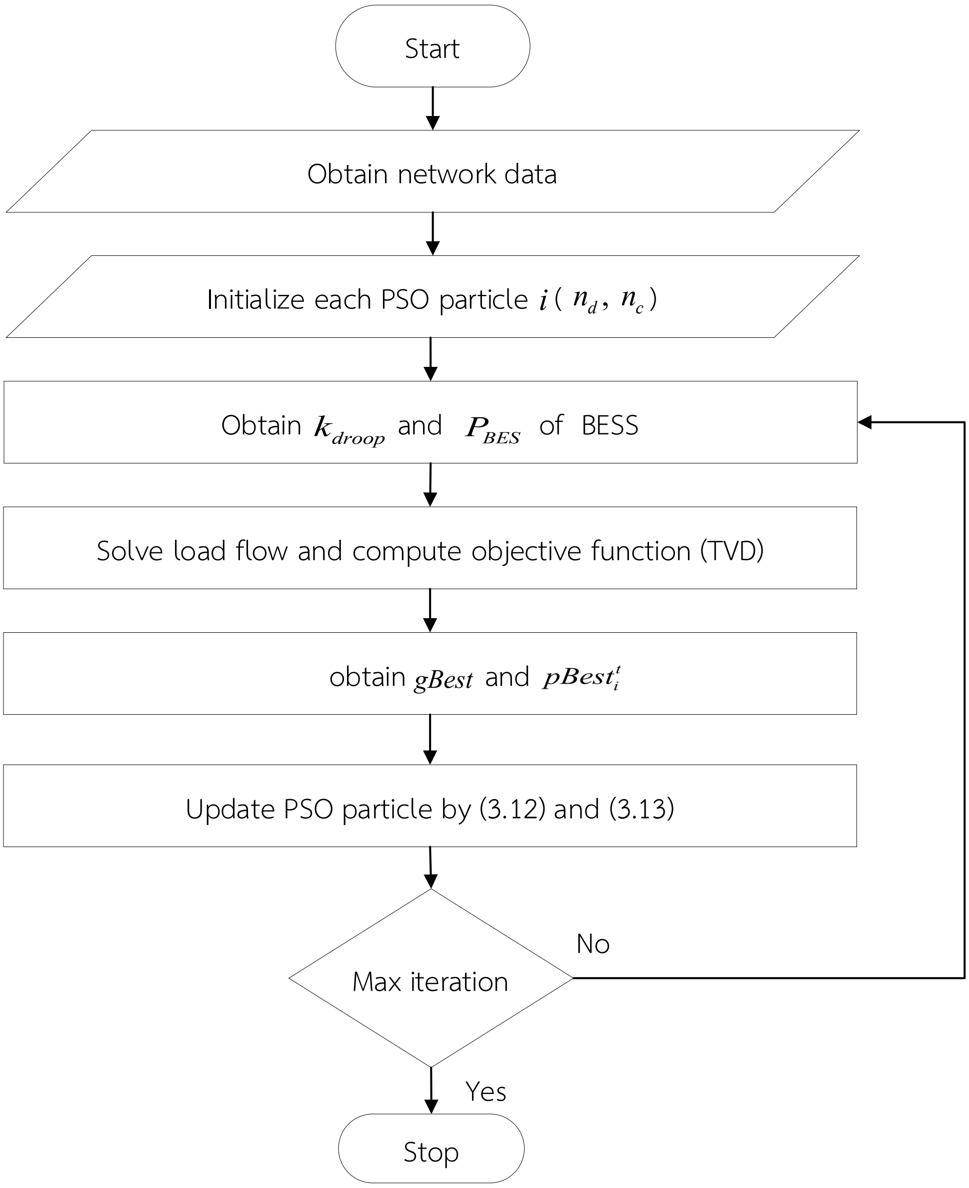

Figure 4.6 The PSO based BESS optimal VDC computation procedure

4.4 BESS Selection Criteria and Sizing

The selection of buses and sizing for BESS installation is based on two main criteria. The bus locations for BESS installation are determined using the L-index, which identifies the buses most susceptible to voltage collapse. These are considered the weakest buses in the system and require the most attention. In the IEEE 33-bus system, there are four branches: Branch 1 includes buses 7–18, Branch 2 includes buses 19–22, Branch 3 includes buses 23–25, and Branch 4 includes buses 26–33. This means that a total of four BESS units are needed. Based on the L-index calculation from table 3.3, the optimal buses for BESS installation are buses 18, 22, 25, and 33, as these have the highest L-index values in each branch. The installation will be considered from the base case only.

The size of each BESS is determined by the total load of each branch. The total loads are as follows: Branch 1 has a total load of 1.075 MW, Branch 2 has 0.36 MW, Branch 3 has 0.93 MW, and Branch 4 has 0.92 MW. For effective voltage control, it is desirable for the BESS to operate continuously, maintaining voltage stability at all times. Therefore, the SoC of the BESS should be set at 0.5, allowing it to absorb energy from PV and wind sources when available, and discharge energy back to the system when generation is low. In this study, the maximum and minimum SoC levels are set at 0.8 and 0.2, respectively, which are considered optimal for BESS operation. This means that only 0.3 p.u. of the SoC is usable, so the BESS capacity must be larger than the total load of each branch. The resulting BESS sizes are as follows: 4.25 MW at bus 18, 1.75 MW at bus 22, 3.5 MW at bus 25, and 3.5 MW at bus 33. The system with renewable energy and BESS is shown on Fig. 4.7.

Similarly, for the IEEE 69-bus system, BESS and renewable energy sources are installed at buses 27, 35, 46, 50, 52, 65, 67, and 69, with capacities of 1.75 MW, 0.5 MW, 0.75 MW, 2.75 MW, 0.25 MW, 5.75 MW, 0.25 MW, and 0.25 MW, respectively, is shown on Fig. 4.8.

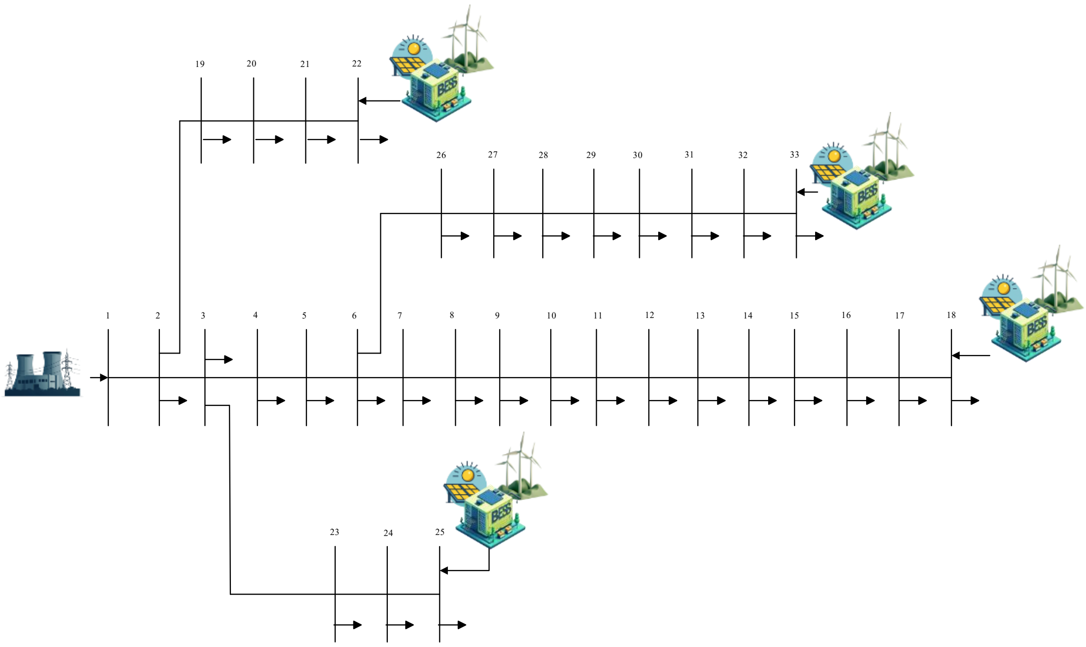

Figure 4.7 The modified IEEE 33-bus with PV and wind power penetration and BESS

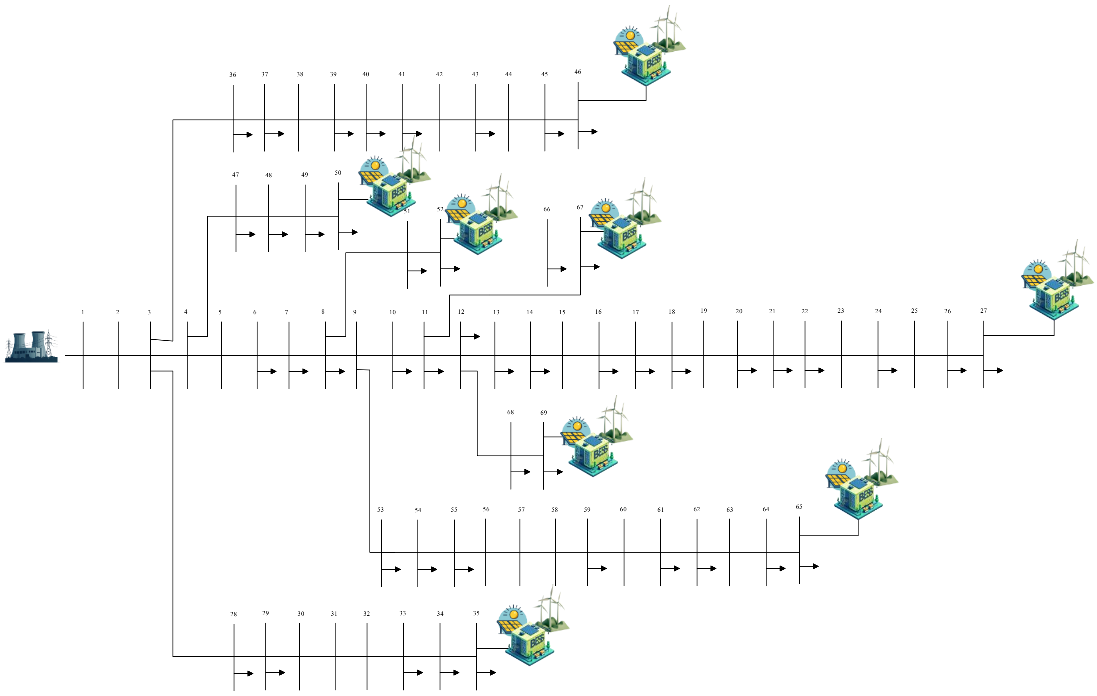

Figure 4.8 The modified IEEE 69-bus with PV and wind power penetration and BESS

In this study, photovoltaic (PV) and wind power, as renewable energy sources, were integrated into the IEEE 33-bus and IEEE 69-bus distribution networks. The sizing of the renewable energy (RE) sources was determined by simulating overvoltage conditions in the power system. This was achieved by incrementally increasing the output of the RE sources and observing whether the voltage magnitude exceeded the specified limit of 1.05 p.u. As a result, the optimal size of the RE sources was found to be 1.25 MW for the IEEE 33-bus system and 1 MW for the IEEE 69-bus system. The PV and wind profiles for these systems are shown in Figure 4.9. (Renewables.ninja).

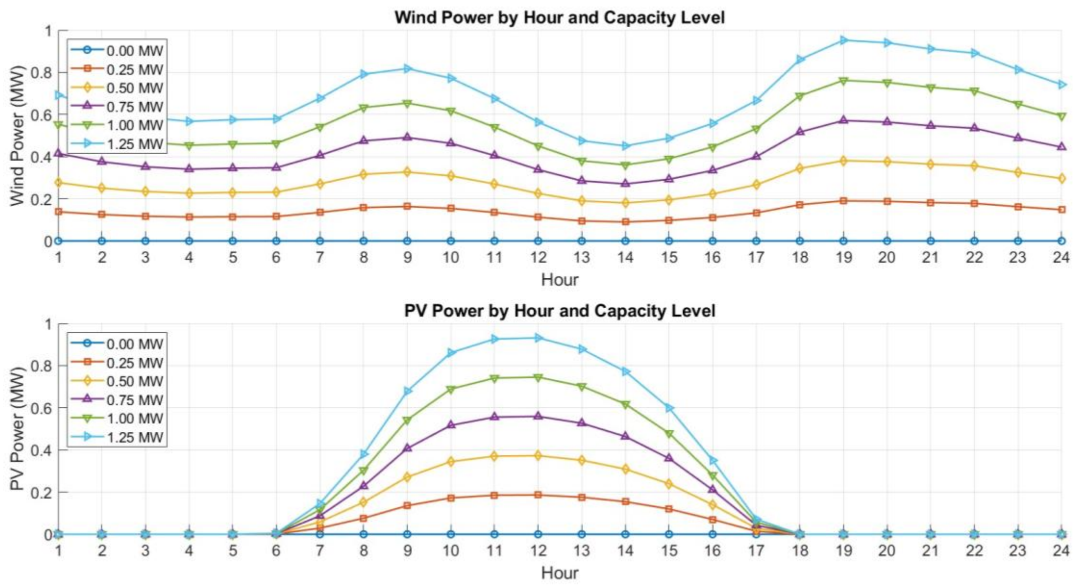

Figure 4.9 The PV and Wind profile 24 hour

4.5 Results and Discussion

The test was conducted on the IEEE 33-bus system, which includes one generator bus and 32 load buses, where bus 1 is designated as the slack bus. The system's voltage restrictions range from 0.95 to 1.05 p.u. The system contains 3.715 MW of real power load and 2.3 MVar of reactive power load. The substation's nominal voltage is configured at 13.8 kV, with the transformer at bus 1 having a capacity of 3 MW.

Table 4.2 also provides the study's parameters, which were evaluated and adjusted as needed, mostly through trial and error. The variable n specifies how quickly the battery can charge or discharge. A larger n allows faster charging or discharging when the BESS SoC is near its maximum or minimum, whereas a smaller n slows charging or discharging when the SoC is near the nominal level. Therefore, we conducted trials to adjust these ranges, as illustrated in Fig 4.5.

The test is divided into three scenarios, as follows:

- case I: IEEE 33-bus base case,
- case II: modified IEEE 33-bus with PV and wind power penetration, and
- case III: modified IEEE 33-bus with PV and wind power penetration and BESS with optimal VDC.

4.5.1 IEEE 33-bus base case.

An initial test was conducted on an IEEE 33-bus distribution system. The voltage of each bus in the system ranges from 0.9038 p.u. to 1.0000 p.u., and the TVD is 1.8047 p.u. This significant deviation indicates that the bus voltages are not within the typical standard range of 0.95 p.u. to 1.05 p.u. The bus with the lowest value is Bus 18. Consequently, the lower-voltage bus should be prioritized to prevent power system instability, which could potentially lead to blackouts.

Table 4.2 Specification of the BESS

Parameter	**Specification**
Range of the adjust exponent (n)	0.1 to 20
The maximum power of battery (P_{BES}^{max})	4.25 MW
The maximum droop coefficient (K_{max})	2182.03
The minimum droop coefficient (K_{min})	0.1
Nominal Voltage (V_0)	1.00 p.u.
Battery capacity (E)	4.25 MWh
The maximum voltage (V_{max})	1.05 p.u.
The minimum voltage (V_{min})	0.95 p.u.

Table 4.2 Specification of the BESS (Continued)

Parameter	Specification
Maximum state of charge ($SoC_{\max}$)	0.8 p.u.
Minimum state of charge ($SoC_{\min}$)	0.2 p.u.

4.5.2 Modified IEEE 33-bus with PV and wind power penetration

In this study, PV and wind power, as renewable energy sources, were integrated into an IEEE 33-bus distribution network. A total of 1.25 MW of PV and wind power was installed at buses 8, 12, 28, and 33. As a result of these renewable energy installations, the system's real power from RE is 6 MW. It was observed that the system voltage ranged from 0.9854 p.u. to 1.0223 p.u. and that TVD was 0.2610 p.u. These findings indicate that high levels of renewable energy penetration affect the power system, causing overvoltages when there is excess power from renewable energy sources and significant voltage fluctuations that negatively affect the electrical network. Therefore, appropriate energy management strategies should be implemented.

4.5.3 Modified IEEE 33-bus with PV and wind power penetration and BESS with optimal VDC.

In case III, the proposed method incorporates a battery into the system and employs PSO to optimize the system to obtain the best value that minimizes TVD. The PSO parameters are configured as follows w ranges from 0.1 to 1.1, both c_1 and c_2 are set to 1.49 and the maximum iterations is 50, which was selected through multiple trial runs. It was observed that the values generally start to converge around 50 iterations, so this value was set accordingly. The results show that the voltage levels on all buses in the system are within the prescribed range, with TVD being 0.2440 p.u. This adjustment was made using the variables presented in Table 4.3, specifically the values of the adjust exponent (n), droop coefficient (k_{droop}) and regulating power (

P_{BES}) for each battery. The sign of P_{BES} for each value indicates whether the battery is charging or discharging. Specifically, a negative sign denotes that the BESS is charging, whereas a positive sign signifies that it is discharging.

Figure 4.10 illustrates the voltage profile for all three scenarios, showing that the proposed method maintains the voltage profile within the specified range through efficient battery charging and discharging. Table 4.4. depicts the 3 scenarios of TVD, indicating that the proposed method also produces the best results by reducing VD compared to case 1 and 2. Furthermore, Fig. 4.11 shows the convergence plot of the proposed PSO-based BESS optimal VDC. it is clear that the value of the objective function progressively converges toward the optimal solution. Fig. 4.12 presents the results of 30 trials conducted using the proposed method that have the average value is 0.2440, standard deviation value is 0.0000, maximum value is 0.2440 and minimum value is 0.2440. The low standard deviation of the objective function values indicates that they are closely clustered, suggesting that the results obtained from PSO algorithm are reliable. The runtime of the proposed method was evaluated over 30 runs on a computer equipped with an AMD Ryzen 5 6600H CPU (3.30 GHz up to 4.50 GHz) and 16 GB of RAM. On average, the method took 54.38 seconds to complete, with a standard deviation of 1.94 seconds. The minimum runtime observed was 52.70 seconds, while the maximum reached 58.28 seconds. Thus, although the PSO method typically requires about 54.38 seconds, it can occasionally take as long as 58.28 seconds, likely due to unfavorable random initializations delaying convergence. These results are illustrated in Figure 4.13.

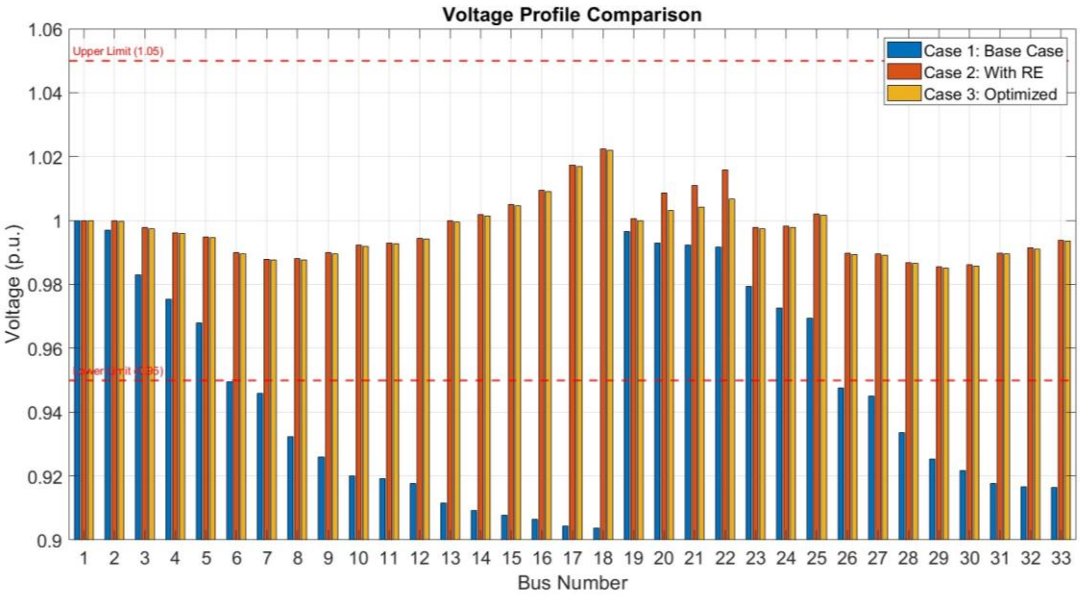

Figure 4.10 Comparative Voltage Profile of modified IEEE 33-bus system

Table 4.3 Adjust exponent, Droop coefficient and BEES regulating power of BESS

Bus with Battery Installed	n	k_{droop}	P_{BES} (MW)	SoC
18	0.1000	0.1031	-0.0023	0.5005
22	20.0000	39.6160	-0.5250	0.8000
25	0.1000	0.1031	-0.0002	0.5001
33	20.0000	39.6160	-0.0000	0.5000

Table 4.4 Adjust exponent, Droop coefficient and BEES regulating power of BESS

Scenarios	TVD (p.u.)
IEEE 33-bus base case	1.8047
Modified IEEE 33-bus with PV and wind power penetration	0.2610
Modified IEEE 33-bus with PV and wind power penetration and BESS with optimal VDC.	0.2440

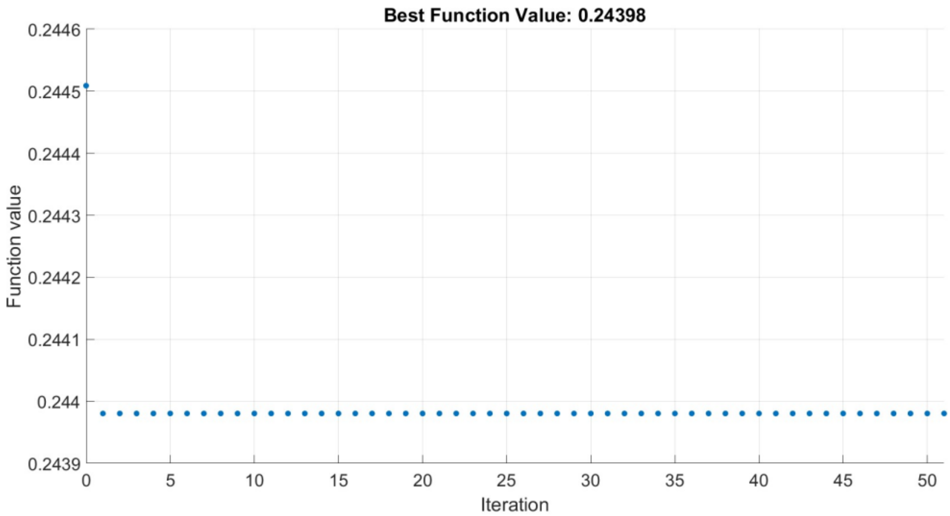

Figure 4.11 the convergence plot of the proposed PSO-based BESS optimal VDC

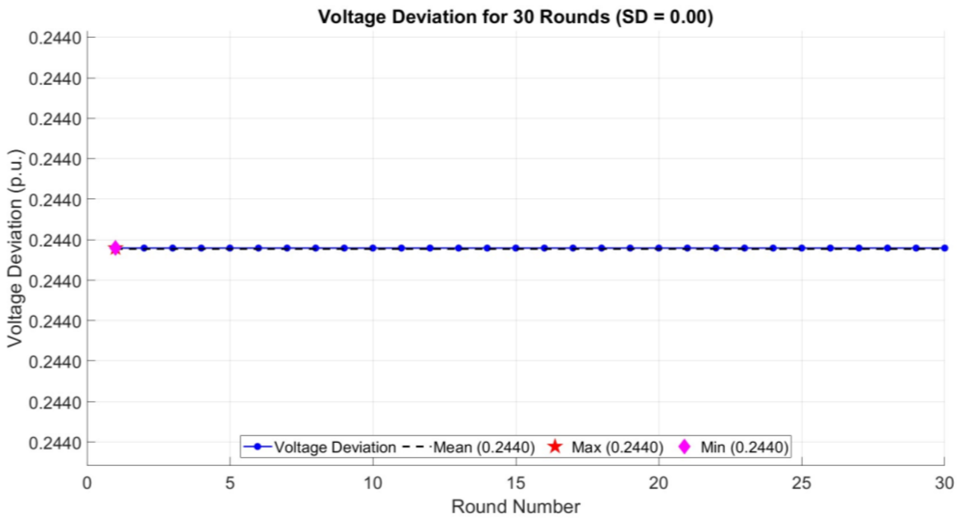

Figure 4.12 the result of 30 trials of the proposed method

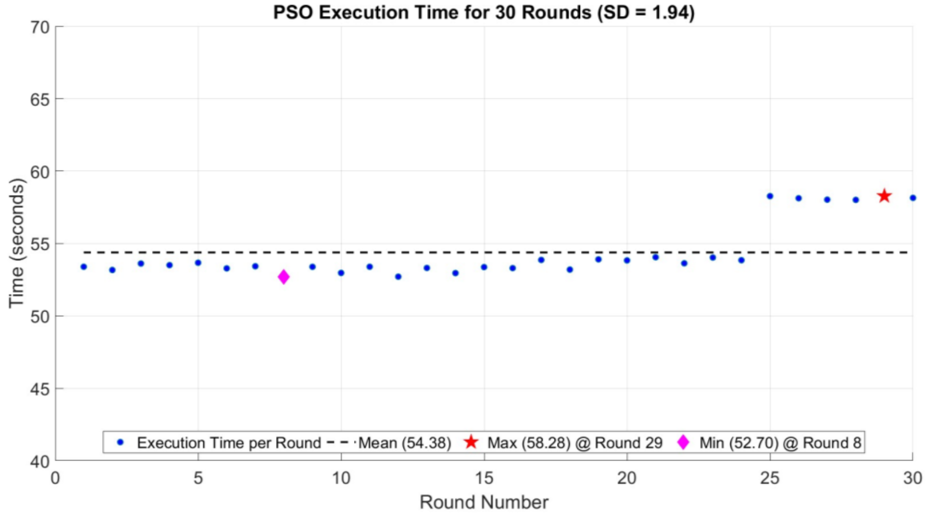

Figure 4.13 The result of 30 trials of the computation time

4.5.4 Sensitivity Analysis of Renewable Energy Placement and Sizing

To further evaluate the robustness and practical applicability of the proposed BESS optimal voltage droop control, this section presents a sensitivity analysis. The primary results demonstrated that the control strategy was highly effective for a specific system configuration, successfully reducing the Total Voltage Deviation (TVD) to 0.2440 p.u. in Case III. However, in real-world distribution networks, the placement and sizing of both Renewable Energy (RE) sources and the BESS units can vary significantly. Therefore, this analysis investigates the performance of the control algorithm when the system configuration deviates from the baseline case. The objective is to determine if the proposed method remains effective under sub-optimal conditions.

To establish the baseline for this analysis, renewable energy, including PV and wind power, was integrated into the IEEE 33-bus distribution system. The configuration includes two 1 MW wind turbine generators on buses 18 and 24; three 1 MW PV systems on buses 5, 21, and 31; and four 500 kW PV systems on buses 8, 12, 28, and 33. Additionally, four 2 MWh BESS units were installed at buses 18, 21, 24, and 32, with their placement determined through a trial-and-error process show in figure

4.14. In this configuration with high RE penetration but without BESS control, the system voltage ranged from 1.0000 p.u. to 1.0534 p.u.

In this scenario, the results show that the voltage levels on all buses in the system are within the prescribed range, with the total voltage deviation (TVD) being 0.0385 p.u. This adjustment was made using the variables presented in Table 4.5, specifically the values of the adjust exponent (n), droop coefficient (k_{droop}), and regulating power (P_{BES}) for each battery.

As shown in Figure 4.15, our proposed method keeps the voltage profile within the required range through efficient battery charging and discharging. Table 4.6 further demonstrates that this method provides the best outcome, reducing voltage deviation more effectively than the other two cases.

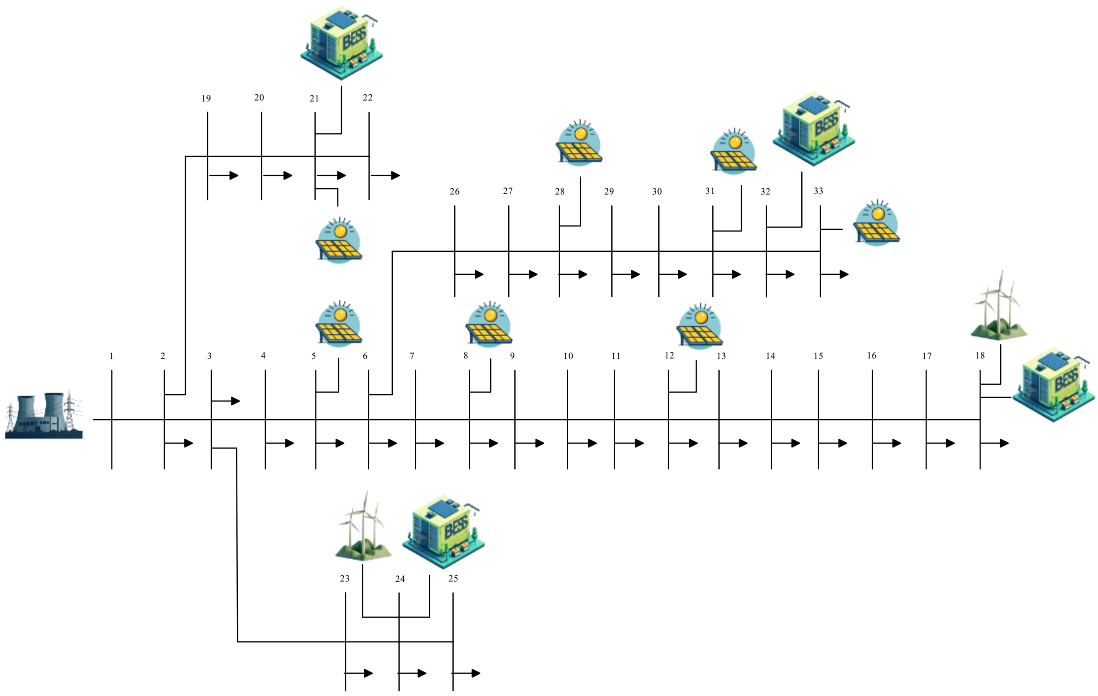

Figure 4.14 The modified IEEE 33-bus with PV and wind power penetration and BESS in sensitivity analysis case

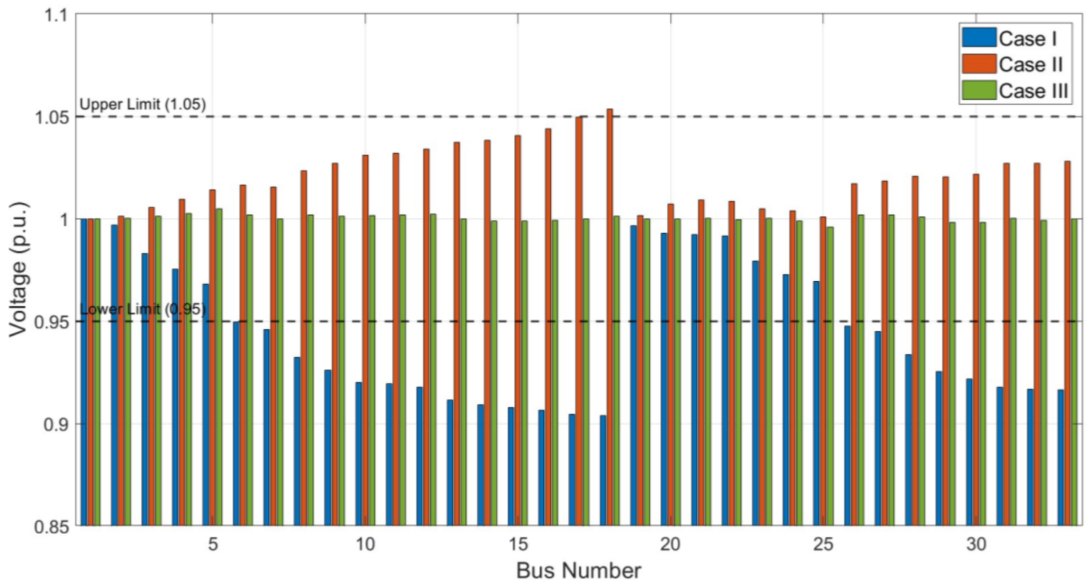

Figure 4.15 Comparative Voltage Profile of modified IEEE 33-bus system in sensitivity analysis case

Table 4.5 Adjust exponent, Droop coefficient and BEES regulating power of BESS in sensitivity analysis case

Bus with Battery Installed	n	k_{droop}	P_{BES} (MW)
18	13.6531	12.3498	-0.6591
22	17.1637	67.4965	-0.6139
25	5.8498	16.0991	-0.0627
33	0.1000	19.5058	-0.5282

Table 4.6 Adjust exponent, Droop coefficient and BEES regulating power of BESS in sensitivity analysis case

Scenarios	TVD (p.u.)
IEEE 33-bus base case	1.8047
Modified IEEE 33-bus with PV and wind power penetration in sensitivity analysis case	0.6879
Modified IEEE 33-bus with PV and wind power penetration and BESS with optimal VDC in sensitivity analysis case	0.0385

4.6 Chapter Summary

This chapter introduces a method for enhancing VS in an active distribution network by installing BESS at weak buses, which were previously identified using the L-index method. The study utilizes an adaptive voltage droop control strategy to manage the BESS, which adjusts its operation based on the battery's SoC to improve efficiency and prevent saturation. To determine the optimal control parameters, PSO is employed to minimize TVD across the system.

The proposed methodology was tested on the IEEE 33-bus system under three scenarios: a base case, a case with high penetration of renewable energy (PV and wind), and a final case that included the BESS with optimized control. The results demonstrated that while the integration of renewables alone caused significant voltage fluctuations, the implementation of the BESS with optimal VDC successfully maintained the voltage profile within the acceptable range of 0.95 to 1.05 p.u. The PSO algorithm proved effective and reliable in finding the optimal parameters, as evidenced by the consistent results over 30 trial runs and the clear convergence of the objective function. A sensitivity analysis further confirmed that the proposed control strategy remains robust and effective even when the placement and sizing of renewable sources and BESS units are altered.